Available online at www.sciencedirect.com

ScienceDirect

Ceramics International 40 (2014) 2529–2534

CERAMICS INTERNATIONAL

www.elsevier.com/locate/ceramint

Short communication

Enhanced energy storage properties of dysprosium doped strontium titanate ceramics

Qi-Guo Hu[a], Zong-Yang Shen[a,b,*], Yue-Ming Li[a], Zhu-Mei Wang[a], Wen-Qin Luo[a], Zhi-Xiang Xie[a]

[a]School of Materials Science and Engineering, Jiangxi Key Laboratory of Advanced Ceramic Materials, Jingdezhen Ceramic Institute, Jingdezhen 333403, China
[b]Materials Research Institute, Pennsylvania State University, University Park, PA 16802, USA

Received 1 June 2013; received in revised form 14 July 2013; accepted 28 July 2013
Available online 2 August 2013

Abstract

Dysprosium doped strontium titanate ceramics of formula $Dy_xSr_{1-1.5x}TiO_3$ (Dy-STO), where $x=0$, 0.01, 0.02, 0.03, and 0.04, were prepared by solid state reaction route. The effect of dysprosium doping amount on structure and dielectric properties of Dy-STO ceramics was investigated. All ceramics are pure cubic perovskite structure, and the lattice parameter decreases with dysprosium doping amount. Scanning electronic microscope (SEM) results show that the grain size is ~30 μm for pure strontium titanate ceramic, while lowered to less than 10 μm after doping dysprosium. Strongly enhanced dielectric constant ($\varepsilon_r=3200$ at 1 kHz) is obtained for Dy-STO ceramics with $x=0.02$, i.e. over 10 times that of pure strontium titanate ceramic ($\varepsilon_r=300$ at 1 kHz). Furthermore, the ε_r shows very stable characteristic under 0~1.92 kV/mm applied bias electric fields. In virtue of low dielectric loss ($\tan\delta<0.03$ at 1 kHz) and high breakdown strength ($E_b>14$ kV/mm), the Dy-STO ceramics are very promising for high voltage capacitors with enhanced energy storage density.

Keywords: A. Sintering; C. Dielectric properties; D. Perovskites; E. Capacitors; Energy storage

1. Introduction

Energy storage ceramic capacitors, which can be made of dielectrics, ferroelectrics and anti-ferroelectrics, are of great importance for a broad range of applications in electrical power systems and modern electronics [1–6]. In recent years, new requirements for compact portable pulsed power applications such as mobile electronic devices, hybrid electric vehicles and switched-mode power supplies are driving the need of ceramic capacitors with enhanced energy storage property [7]. In general, the volumetric energy density γ of a linear dielectric is directly proportional to relative dielectric constant ε_r while the square of applied electric field E, i.e., $\gamma=0.5\varepsilon_r\varepsilon_0E^2$, where ε_0 ($=8.85\times10^{-12}$ F/m) is the vacuum dielectric permittivity. As a result, large relative dielectric constant ε_r and high electrical breakdown strength E_b are two essential factors to achieve high energy storage density. Furthermore, low dielectric loss is also an important factor for practical usages. Previous work almost mainly focused on enhancing breakdown strength E_b of the ceramics because an applied electric field E makes a more pronounced contribution to energy storage density [8–11]. However, it should be pointed out that increasing ε_r is critical to compact pulsed power applications, since a higher ε_r can lead to a shorter length of pulse forming lines [12].

Among the ceramic candidates, strontium titanate ($SrTiO_3$, STO), which shows a linear characteristic and has a medium high ε_r (~300), as well as relatively strong E_b (~10 kV/mm), is one of the most promising dielectric materials for energy storage capacitors. In order to increase ε_r and/or E_b and then obtain higher possible storing energy per unit volume, impurity doped STO ceramics have been extensively studied. During the past several decades, isovalent ions modified STO, i.e., divalent Ba^{2+}, Ca^{2+}, Pb^{2+} substituting for A-site Sr^{2+}, as well as tetravalent Zr^{4+} for B-site Ti^{4+}, was widely studied and reported to result in preferable enhanced energy storage property for high voltage capacitors [13–16]. On the other hand, non-isovalent ions, especially trivalent ions doped STO

*Corresponding author at: School of Materials Science and Engineering, Jiangxi Key Laboratory of Advanced Ceramic Materials, Jingdezhen Ceramic Institute, Jingdezhen 333403, China. Tel.: +86 798 8499678; fax: +86 798 8491446.
E-mail addresses: shenzongyang@gmail.com, shenzongyang@163.com (Z.-Y. Shen).

0272-8842/$ - see front matter © 2013 Elsevier Ltd and Techna Group S.r.l. All rights reserved.
http://dx.doi.org/10.1016/j.ceramint.2013.07.126

ceramics have been attracted much attention in recent years due to their some distinctive characteristics. For example, Tkach et al. observed an enhancement of tetragonality in trivalent rare earth (La^{3+}, Gd^{3+}, and Y^{3+}) doped STO ceramics by Raman spectra [17]. Shi et al. reported that Er^{3+} ions are gradually transferred from A- to B-site by increasing ratio of Sr/Ti in STO, and the light-response range effectively extends from the ultraviolet rays to the visible-light for photocatalytics [18]. Most interestingly, Chen and Zhi obtained a "giant" dielectric constant ($\varepsilon_r \sim 10^4$) in trivalent Bi^{3+} doped STO ceramics, but this ceramic with "giant" ε_r is unfortunately pointed out to be useless in making capacitors for energy storage due to its high dielectric loss [19]. Meanwhile, the volatilization of bismuth in high sintering temperature makes a drawback for the preparation and later deep analysis of the ceramics.

Based on the above considerations, our work has been concentrating on non-volatile trivalent rare earth ions modified STO ceramics. More recently, we successfully fabricated Nd^{3+} doped STO ceramics with both high ε_r ($\sim 10^4$) and strong E_b (>10 kV/mm) by equal mole substituting trivalent Nd^{3+} for divalent Sr^{2+} [20]. It is unfortunate that this ceramic also has relatively high dielectric loss (~ 0.1 at 1 kHz). In this work, however, rare earth dysprosium is selected to modify STO. Of particular importance is that A-site strontium vacancies are introduced in advance for compensating the charge unbalance induced by trivalent Dy^{3+} substituting for divalent Sr^{2+}, i.e., $Dy_xSr_{1-1.5x}TiO_3$ similar to $[M_xSr_{1-1.5x}(V_{Sr})_{0.5x}]TiO_3$ (M=La^{3+}, Gd^{3+}, Y^{3+}) reported by Tkach et al. and $Bi_xSr_{1-1.5x}TiO_3$ by Chen and Zhi [17,19]. The effect of Dy doping amount on the structure and dielectric energy storage property of the ceramics is investigated.

2. Experimental procedures

Reagent-grade $SrCO_3$ (99%), TiO_2 (98%), and Dy_2O_3 (99.9%) were used as raw materials to fabricate $Dy_xSr_{1-1.5x}TiO_3$ (Dy-STO) ceramics *via* solid state reaction method, where x=0, 0.01, 0.02, 0.03, and 0.04. The raw materials were weighed according to the stoichiometric composition of Dy-STO with different x values, and then mixed by planet ball milling for 6 h in a nylon bottle with deionized water and zirconia balls. The mixed slurry were dried and calcined at 1100 °C for 3 h in an alumina crucible. The calcined powders were planet ball milled again for 6 h, dried and granulated with polyvinyl alcohol (PVA) as a binder, then pressed into disks of 12 mm diameter and about 1.3 mm thick under 120 ± 10 MPa. The disks were preheated in air at 650 °C for 1 h to remove organic binders and finally sintered at 1350 °C for 3 h in air with a heating rate of 3 °C/min and furnace-cooled to ambient temperature.

X-ray diffraction (XRD: X' Pert Pro PANalytical, Cu-$K\alpha$ radiation) was performed to characterize the phase structure of sintered ceramic samples at room temperature. The lattice parameters were precisely calculated using X'Pert HighScore software according to XRD profiles. The microstructure feature of polished and thermally etched surfaces of sintered ceramics was characterized by a field emission scanning electron microscopy (FE–SEM, JSM-5610LV; JEOL, Japan).

The ceramic samples were carefully polished to about 1 mm thick for dielectric measurements, while about 0.6 mm thick for bias electric field test. Silver pastes were painted on both sides of polished ceramic samples, and then fired to electrodes at 650 °C for 30 min. Room temperature relative dielectric constant ε_r and dielectric loss $\tan\delta$ were measured by a precision impedance analyzer (HP4294A, Agilent) at 1 kHz. The temperature dependence of the ε_r and $\tan\delta$ was determined using a LCR meter (HP4284, Agilent) in a range from −70 °C to 180 °C, being connected to a computer controlled temperature chamber (Delta design 2300). Breakdown strength measurements were performed using a breakdown strength testing instrument (JJC9906-A, Wuhan Xinghuo Electrical Equipment Co., China) in silicone oil medium to avoid arcing. An AC voltage ramp of about 1 kV/s was applied to the sample until the dielectric breakdown occurs. For each composition, an average electrical breakdown strength E_b was obtained from at least 6 specimens testing. The relationship between ε_r and bias electric fields was conducted using a bias electric field testing system (FMRL, Tongji University, China) at the measuring frequency of 1 kHz.

3. Results and discussion

Fig. 1 shows the XRD patterns of Dy-STO ceramics with different x values in the 2θ range from 20° to 80°. It can be seen from Fig. 1 that all Dy-STO ceramics possess a single cubic perovskite structure without any traced secondary phases. Moreover, as observed from the inset of Fig. 1, the (200) diffraction peak shifts to higher angle with the increase of x value. These results indicate that the rare earth dysprosium must be incorporated into the host lattice of the perovskite structure, and experimentally demonstrate that Sr cation vacancies charge compensation mechanism is available in this

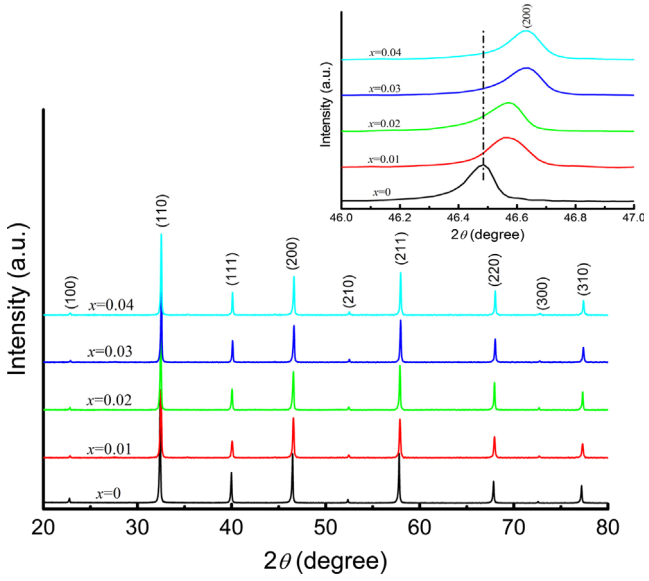

Fig. 1. XRD patterns of Dy-STO ceramics.

Table 1
Composition, structure, lattice parameters of the Dy-STO ceramics.

Composition (x)	Structure	Lattice parameter (Å) $a=b=c$	Unit-cell volume (Å^3)
0	Cubic	3.9049	59.54
0.01	Cubic	3.9000	59.32
0.02	Cubic	3.8986	59.26
0.03	Cubic	3.8950	59.09
0.04	Cubic	3.8941	59.05

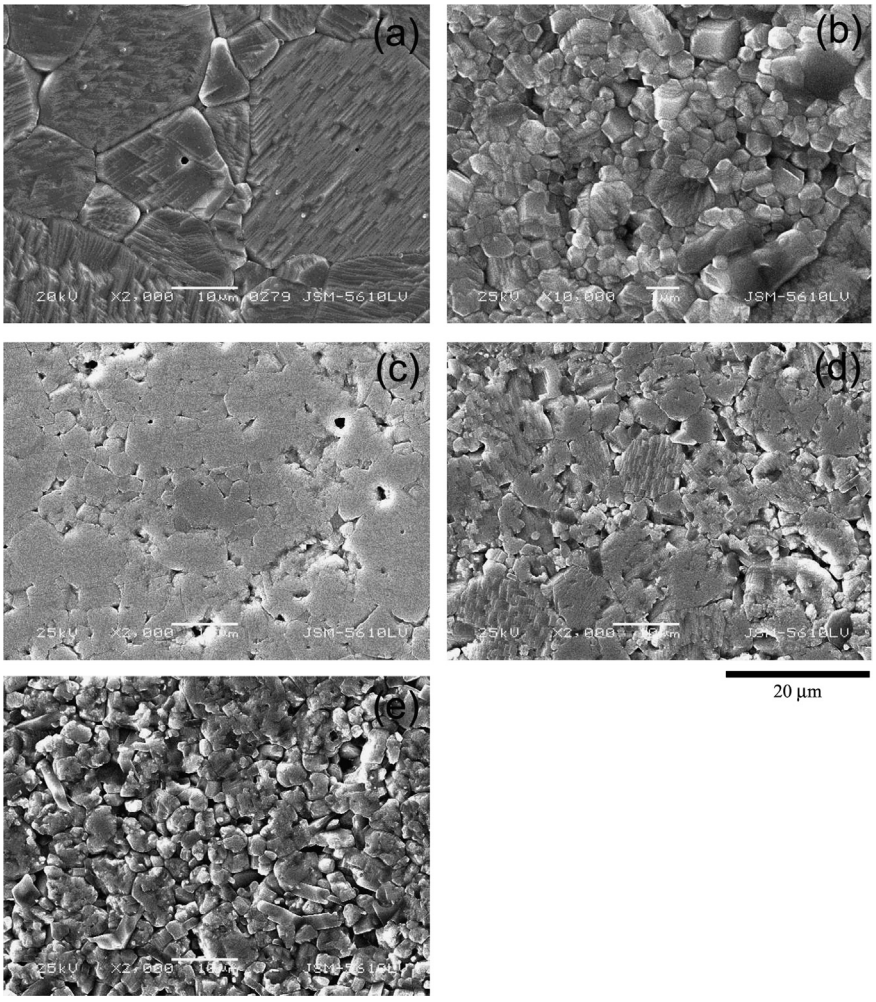

Fig. 2. SEM images of polished and thermally etched surfaces of Dy-STO ceramics: (a) $x=0$; (b) $x=0.01$; (c) $x=0.02$; (d) $x=0.03$; and (e) $x=0.04$.

work. The calculated lattice parameters of Dy-STO ceramics are given in Table 1. For pure STO ($x=0$), a cubic cell with lattice parameter $a=3.9049$ Å is indexed, in good agreement with the reference data of $a=3.905$ Å [21]. As also reported in Table 1, the lattice parameter gradually decreases with increasing x value, which is owing to the shrinkage of unit cell induced by ionic radius of Dy^{3+} ($r_i=1.18$ Å, CN=12) smaller than that of Sr^{2+} ($r_i=1.44$ Å, CN=12). Here we should note that the ionic radius of Dy^{3+} in 12 coordinate is based on the relationship between coordination number and effective ionic radii after Shannon's table (see Fig. 2 in Ref# [22]). Of course, the existence of Sr vacancies should also make a little contribution to the shrinkage of the unit cell volume.

Fig. 2 shows SEM images of polished and thermally etched surfaces of Dy-STO ceramics with different x values. The grain size is found to be ~30 μm for pure STO ceramics from Fig. 2(a), consistent with that reported by Tkach et al. [23]. After doping dysprosium, the grain size can be markedly suppressed to about several micrometers according to Fig. 2 (b–d). This phenomenon suggests that dysprosium doping inhibits the grain growth of the ceramics. Actually, rare earth often plays a grain growth inhibitor role in the fabrication of some fine ceramics [24,25].

Table 2
The dielectric properties of Dy-STO ceramics.

Composition (x)	ε_r (@ 1 kHz)	tan δ (@ 1 kHz)	E_b (kV/mm)
0	300	0.002	9.9
0.01	760	0.029	16.4
0.02	3200	0.026	16.2
0.03	2400	0.022	15.2
0.04	1970	0.024	14.5

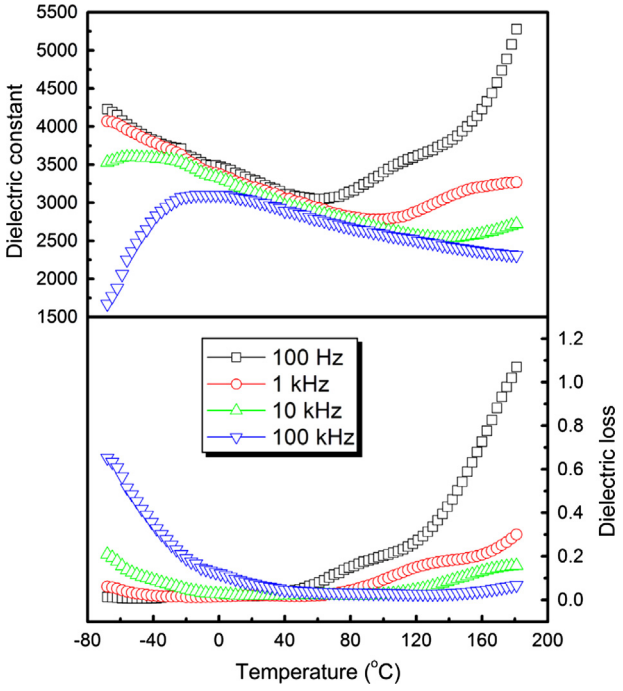

Fig. 3. The dielectric constant and loss of Dy-STO ceramics with $x=0.02$ as a function of temperature from −70 °C to 180 °C.

Table 2 lists the dielectric properties of Dy-STO ceramics with different x values. As compared to pure STO ceramics ($x=0$), the ε_r and E_b are overall improved after doping dysprosium. Especially for Dy-STO ceramic with $x=0.02$, the ε_r significantly increases to 3200, which exceeds 10 times that of pure STO. In order to explain the significant enhancement of ε_r after doping dysprosium, the possible defect structures in Dy-STO ceramics should be considered. In this work, the Sr cation vacancies are introduced in advance for compensating charge unbalance induced by trivalent Dy^{3+} substituting for divalent Sr^{2+}, which can be described as the following defect reaction Eq. (1):

$$Dy_2O_3 + 3TiO_2 \rightarrow 2Dy_{Sr}^{\bullet} + 3Ti_{Ti}^{x} + 9O_O^{x} + V_{Sr}^{''} \quad (1)$$

Previously, Burn et al. reported that the cation vacancies charge compensation mechanism is predominant for donor doped STO ceramics as the donor concentration greater than 0.2 mol% [26]. In this work, the lowest dysprosium doping concentration is 1 mol%, much higher than 0.2 mol%, demonstrating Sr vacancies charge compensation mechanism should be available. Therefore, according to Eq. (1), the charged donor defects ($Dy_{Sr}^{\bullet}$) are suggested to be wholly compensated by strontium vacancies ($V_{Sr}^{''}$). Under this situation, the positive and negative charge centers will attract each other to form defect dipoles as ($Dy_{Sr}^{\bullet}-V_{Sr}^{''}$), and the defect dipoles can respond to an external electric field, making contribution to the enhancement of the dielectric constant. Moreover, the crystal structure and microstructure should affect the polarization behavior of defect dipoles under external electric fields. The highest ε_r value for the composition of $x=0.02$ should be associated with the combined effect of crystal and micro structures, which induces the optimized defect dipoles polarization at this composition. As also shown in Table 2, it is important to note that the tan δ of Dy-STO ceramics is lower than 0.03, meeting the requirement of making energy storage capacitors. Furthermore, the average breakdown strength E_b of all Dy-STO ceramics surpasses 14 kV/mm, which increases by 50% comparing with that of pure STO ceramic ($x=0$). The overall enhancement of E_b for Dy-STO ceramics should be due to the suppressed grain size after doping dysprosium (see Fig. 2(b–d)), since it has been confirmed that small and homogeneous grain size will enhance the breakdown strength of the ceramics [10,12].

Fig. 3 shows the dielectric constant and loss of Dy-STO ceramics with $x=0.02$ as a function of temperature from −70 °C to 180 °C. A dielectric dispersion can be detected around 120 °C, where the dielectric properties are strongly suppressed with the increase of measuring frequencies. This phenomenon supports the existing of defect dipoles in Dy-STO ceramics, and the relaxation of defect dipoles at elevated temperatures should contribute to the observed dielectric dispersion.

Fig. 4 shows the ε_r of Dy-STO ceramics as a function of bias electric fields. It can be seen that the ε_r shows nearly field-independent characteristic, regardless of increasing or decreasing bias electric fields. Such good stability of ε_r versus bias electric field is very beneficial to high voltage capacitors.

The energy storage density γ of Dy-STO ceramics is calculated according to $\gamma=0.5\varepsilon_r\varepsilon_0E^2$ and shown in Fig. 5, using the applied bias electric field E and corresponding ε_r data in Fig. 4. Owing to the linear characteristic of ε_r versus bias electric field (see Fig. 4), the experimental data of the energy storage density with the applied bias electric field can be well fitted to quadratic parabola function by least squares method. For example, the fitting curve equation is $\gamma=0.0139E^2$ for Dy-STO ceramic with $x=0.02$. Predictably, this Dy-STO

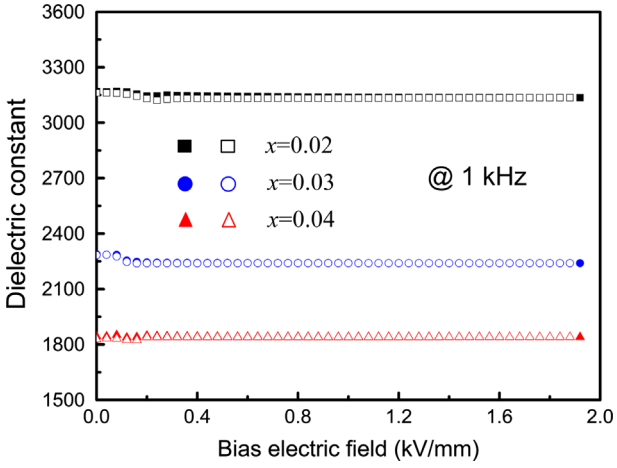

Fig. 4. The ε_r of Dy-STO ceramics as a function of bias electric field. Filled pattern: increasing bias and open pattern: decreasing bias.

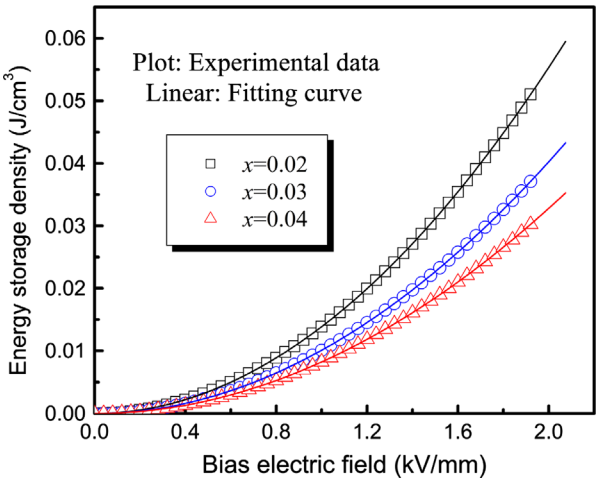

Fig. 5. The energy storage density of Dy-STO ceramics under different bias electric fields.

ceramic has great potential to fabricate thick films for high voltage multilayer capacitors with enhanced energy storage density.

4. Conclusions

Trivalent rare earth Dy^{3+} doped strontium titanate ceramics with single cubic perovskite structure are successfully prepared by solid state reaction route. Introducing Sr vacancies in advance for charge compensation is experimentally available in this work. Strongly enhanced $\varepsilon_r = 3200$ at 1 kHz is obtained in $Dy_{0.02}Sr_{0.97}TiO_3$ ceramics, and the ε_r presents nearly bias electric field independent characteristic. Moreover, both low tan δ (0.026 at 1 kHz) and high E_b (16.2 kV/mm) are also achieved, making the $Dy_{0.02}Sr_{0.97}TiO_3$ ceramic promising candidate for energy storage capacitors in high voltage conditions.

Acknowledgments

This work was financially supported by the National Natural Science Foundation of China (Grant nos. 51102121 and 51262011), the Natural Science Foundation of Jiangxi Province of China (Grant no. 20114BAB216020) and the Doctorate Foundation of Jingdezhen Ceramic Institute (Grant no. 006000345). The author (Z. Y. Shen) also would like to thank the support of China Scholarship Council.

References

[1] D.P. Shay, N.J. Podraza, N.J. Donnelly, C.A. Randall, High energy density, high temperature capacitors utilizing Mn-doped $0.8CaTiO_3$–$0.2CaHfO_3$ ceramics, Journal of the American Ceramic *So*ciety 95 (2012) 1348–1355.

[2] N. Ortega, A. Kumar, J.F. Scott, B.C. Douglas, M. Tomazawa, K. Shalini, D.G.B. Diestra, R.S. Katiyar, Relaxor-ferroelectric superlattices: high energy density capacitors, Journal of Physics: Condensed Matter 24 (2012) 445901.

[3] F. Gao, X. Dong, C. Mao, W. Liu, H. Zhang, L. Yang, F. Cao, G. Wang, J. Jones, Energy-storage properties of $0.89Bi_{0.5}Na_{0.5}TiO_3$–$0.06BaTiO_3$–$0.05K_{0.5}Na_{0.5}NbO_3$ lead-free anti-ferroelectric ceramics, Journal of the American Ceramic *So*ciety 94 (2011) 4382–4386.

[4] Q. Zhang, Y. Zhang, X. Wang, T. Ma, Z. Yuan, Influence of sintering temperature on energy storage properties of $BaTiO_3$–$(Sr_{1-1.5x}Bi_x)TiO_3$ ceramics, Ceramics International 38 (2012) 4765–4770.

[5] S. Jiang, L. Zhang, G. Zhang, S. Liu, J. Yi, X. Xiong, Y. Yu, J. He, Y. Zeng, Effect of Zr:Sn ratio in the lead lanthanum zirconate stannate titanate anti-ferroelectric ceramics on energy storage properties, Ceramics International 39 (2013) 5571–5575.

[6] Y. Zhang, J. Huang, T. Ma, X. Wang, C. Deng, X. Dai, Sintering temperature dependence of energy-storage properties in $(Ba,Sr)TiO_3$ glass-ceramics, Journal of the American Ceramic *So*ciety 94 (2011) 1805–1810.

[7] M. Fazio, H. Kirbie, Ultracompact pulsed power, Proceedings of the IEEE 92 (2004) 1197–1204.

[8] X. Wang, Y. Zhang, X. Song, Z. Yuan, T. Ma, Q. Zhang, C. Deng, T. Liang, Glass additive in barium titanate ceramics and its influence on electrical breakdown strength in relation with energy storage properties, Journal of the European Ceramic Society 32 (2012) 559–567.

[9] J. Huang, Y. Zhang, T. Ma, H. Li, L. Zhang, Correlation between dielectric breakdown strength and interface polarization in barium strontium titanate glass ceramics, Applied Physics Letters 96 (2010) 042902.

[10] A. Young, G. Hilmas, S.C. Zhang, R.W. Schwartz, Effect of liquid-phase sintering on the breakdown strength of barium titanate, Journal of the American Ceramic *So*ciety 90 (2007) 1504–1510.

[11] T. Wu, Y. Pu, K. Chen, Dielectric relaxation behavior and energy storage properties in $Ba_{0.4}Sr_{0.6}Zr_{0.15}Ti_{0.85}O_3$ ceramics with glass additives, Ceramics International 39 (2013) 6787–6793.

[12] Y. Ye, S. Zhang, F. Dogan, E. Schamiloglu, J. Gaudet, P. Castro, M. Roybal, M. Joler, C. Christodoulou, Influence of nanocrystalline grain size on the breakdown strength of ceramic dielectrics, in: Proceedings of the 14th IEEE International Pulsed Power Conference, PPC-2003, 1, 2003, pp. 719–722.

[13] R. Shende, D. Kruegera, S. Lombardo, Solid state synthesis, processing, and electrical properties of $Sr(Ti_xZr_{1-x})O_3$ $(0 \le x \le 1)$ ceramics for high voltage applications, Journal of Ceramic Processing Research 4 (2003) 191–196.

[14] G. Triani, A. Hilton, B. Ricketts, Dielectric energy storage in $Pb_xSr_{1-x}TiO_3$ ceramics, Journal of Materials Science: Materials in Electronics 12 (2001) 17–20.

[15] B. Ricketts, G. Triani, A. Hilton, Dielectric energy storage densities in $Ba_{1-x}Sr_xTi_{1-y}Zr_yO_3$ ceramics, Journal of Materials Science: Materials in Electronics 11 (2000) 513–517.

[16] S. Nishigaki, K. Murano, A. Ohkoshi, Dielectric properties of ceramics in the system $(Sr_{0.50}Pb_{0.25}Ca_{0.25})TiO_3$–$Bi_2O_3 \cdot 3TiO_2$ and their applications in a high-voltage capacitor, Journal of the American Ceramic *So*ciety 65 (1982) 554–560.

[17] A. Tkach, A. Almeida, J.A. Moreira, T.M. Correia, M.R. Chaves, O. Okhay, P.M. Vilarinho, I. Gregora, J. Petzelt, Enhancement of tetragonality and role of strontium vacancies in heterovalent doped $SrTiO_3$, Applied Physics Letters 98 (2011) 052903.

[18] J. Shi, J. Ye, L. Ma, S. Ouyang, D. Jing, L. Guo, Site-selected doping of upconversion luminescent Er^{3+} into $SrTiO_3$ for visible-light-driven photocatalytic H_2 or O_2 evolution, Chemistry—A European Journal 18 (2012) 7543–7551.

[19] C. Ang, Z. Yu, High capacitance-temperature sensitivity and giant dielectric constant in $SrTiO_3$, Applied Physics Letters 90 (2007) 202903.

[20] Z.Y. Shen, Y.M. Li, W.Q. Luo, Z.M. Wang, X.Y. Gu, R.H. Liao, Structure and dielectric properties of $Nd_xS_{1-x}TiO_3$ ceramics for energy storage application, Journal of Materials Science: Materials in Electronics 24 (2013) 704–710.

[21] JCPDF, Card no. 35-0734.

[22] R. Shannon, Revised effective ionic radii and systematic studies of interatomic distances in halides and chalcogenides, Acta Crystallographica A 32 (1976) 751–767.

[23] A. Tkach, P.M. Vilarinho, A.L. Kholkin, Structure-microstructure-dielectric tunability relationship in Mn-doped strontium titanate ceramics, Acta Materialia 53 (2005) 5061–5069.

[24] H. Kishi, N. Kohzu, J. Sugino, H. Ohsato, Y. Iguchi, T. Okuda, The effect of rare-earth (La, Sm, Dy, Ho and Er) and Mg on the microstructure in $BaTiO_3$, Journal of the European Ceramic *So*ciety 19 (1999) 1043–1046.

[25] D. Gao, K. Kwok, D. Lin, H. Chan, Microstructure and electrical properties of La-modified $K_{0.5}Na_{0.5}NbO_3$ lead-free piezoelectric ceramics, Journal of Physics D*:* Applied Physics 42 (2009) 035411.

[26] I. Burn, S. Neirman, Dielectric properties of donor-doped polycrystalline $SrTiO_3$, Journal of Materials Science 17 (1982) 3510–3524.